Polar Meteorol. Glaciol., **19**, 1–14, 2005

Isotopic fractionation of water during snow formation: Experimental evidence of kinetic effect

Ryu Uemura[1,2*†], Yohei Matsui[2], Naohiro Yoshida[1,2], Osamu Abe[3] and Shigeto Mochizuki[3]

[1]*Department of Environmental Science and Technology, Tokyo Institute of Technology, Yokohama 226-8502*
[2]*SORST Project, Japan Science and Technology Corporation, Kawaguchi 332-0012*
[3]*Snow and Ice Research Group, National Research Institute for Earth Science and Disaster Prevention, Shinjo 996-0091*
[*]*Now at National Institute of Polar Research, Kaga-1chome, Itabashi-ku, Tokyo 173-8515*
[†]*Corresponding author. E-mail: ruemura@pmg.nipr.ac.jp*

(Received February 18, 2005; Accepted June 29, 2005)

Abstract: Deuterium excess (d-excess $=\delta D-8\cdot\delta^{18}O$), which is calculated using two water isotope ratios (δD and δ^{18}O), is an indicator of kinetic isotope fractionation. The d-excess value reflects the evaporation process from the ocean or ice-crystal growth. Consequently, d-excess records preserved in ice cores may provide a climatic history of ocean surface conditions at the vapor source area. J. Jouzel and L. Merlivat (J. Geophys. Res., **89**, 11749, 1984) proposed an isotope model to analyze information from ice cores. That model includes kinetic fractionation during snow formation, depending on the degree of the supersaturation ratio of vapor. However, no experiment was conducted under the controlled supersaturation ratio. Experiments described herein measured the isotopic ratios of the vapor and artificial snow produced under a controlled supersaturation ratio to confirm the kinetic isotope effect experimentally. Results indicate a higher d-excess value for ice crystals at a higher vapor supersaturation ratio and provide experimental evidence for the kinetic effect during snow formation.

key words: water isotope, kinetic fractionation, artificial snow, deuterium excess

1. Introduction

Stable isotope ratios of water in the ice core reflect past variations in climate. Hydrogen and oxygen isotopes of water are commonly used as indicators of surface air temperatures. Isotope ratios are expressed using delta notation as follows: $\delta D=\{[(D/H)_{sample}/(D/H)_{VSMOW}]-1\}$, $\delta^{18}O=\{[(^{18}O/^{16}O)_{sample}/(^{18}O/^{16}O)_{VSMOW}]-1\}$. On the other hand, an indicator obtained by combining δD and δ^{18}O, deuterium excess ($=\delta D-8\cdot\delta^{18}O$) (Dansgaard, 1964) provides information related to ocean surface conditions at the area of origin of water vapor. Recently, climatic records of deuterium excess (hereafter referred to as *d* or d-excess) containing full glacial-interglacial cycles have been obtained from ice cores drilled in the Antarctic ice sheet (Vimeux *et al.*, 2001;

Watanabe *et al*., 2003). These records are useful for comparing the Antarctic air temperature and fluctuation in ocean surface temperatures in the Southern Hemisphere (Stenni *et al*., 2001; Uemura *et al*., 2004).

Isotope fractionations of water include two physical processes: equilibrium isotope fractionation and kinetic isotope fractionation. Equilibrium fractionation and kinetic fractionation are indicated respectively as δD (or δ^{18}O) and d. Equilibrium isotope fractionation is caused by the difference in saturation vapor pressure of the isotopic molecular species. On the other hand, kinetic isotope fractionation results from the difference in molecular diffusivities. In keeping with the general terminology of water isotope studies, the isotope effect caused by molecular-diffusive transport is called *kinetic isotope effect* in this study. The isotope effect, because of the difference in reaction rates, is also typically termed as *kinetic effect* in geochemical studies.

Jouzel and Merlivat (1984) proposed an isotope model that includes kinetic isotope fractionation from vapor to ice depending on the degree of the supersaturation ratio over ice. This isotope model of snow formation is widely used in ice core analyses to interpret the Antarctic d record as a climatic history of vapor source region. However, their study performed only the isotopic measurement of the frost grown on a cooling plate (-20°C) set at room temperature (20°C); no experiment was conducted under conditions that controlled the supersaturation ratio. One difficulty encountered in conducting such a study is that the artificial-snow-producing experimental apparatus (Nakaya, 1951) is too small to obtain an adequate amount of vapor sample, which is required for isotopic measurement, without disturbing the experimental system.

In the present study, to confirm the kinetic isotope effect experimentally during ice crystal growth, we measured the isotopic ratios of the source vapor and artificial snow, which were produced under controlled air temperature and the supersaturation ratio of vapor. The experimental equipment used in this study generates a large amount of snow (maximum snow production, 19 kg h^{-1}) (Higashiura *et al*., 1997). Therefore, sampling of snow and vapor for isotope measurement is possible without disturbing the system. The experimental temperature around the snow formation device ranged from -19°C to -14°C with air circulation. We compared the experimental and theoretical values obtained from calculations for the isotopic ratio changes between vapor and ice crystals. Both results indicate a higher d value for the ice crystals at a higher vapor supersaturation ratio and provide experimental evidence for the kinetic effect during snow formation.

2. Method

2.1. Experimental apparatus

The experiment was conducted using a snowfall device; it generates frost that resembles natural snow in large quantities (Cryospheric Environment Simulator, National Research Institute for Earth Science and Disaster Prevention, Yamagata, Japan). The experimental apparatus was installed in a three-story low-temperature room (Fig. 1a). Water is supplied from a water tank (210 L) to water pans at a constant rate. Subsequently, it circulates through the pans. The water in the water pans is evaporated by a constant wind; water vapor is supplied to the snow-forming membranes. The

membranes have gas permeability. Such characteristics of the membranes maintain adequate ventilation around artificial snow to prevent an increase in temperatures resulting from the latent heat of sublimation. Adjusting the water temperature in the water pans controls the evaporation rate. Water vapor, the evaporate from the evaporating pan, passes through the snow-forming membranes and generates ice crystals on their surfaces. Twelve membranes (height, 2.0 m; width, 3.0 m; two-ways; total area, 144 m^2) are rotated with the conveyor belt-like units. Using piano wire, the generated ice crystals are detached from the membrane at the bottom of the snow formation apparatus. The detached crystals fall downward, as "snow", 9.6 m and accumulate on the snowfall table (5.0 m × 3.0 m).

Conditions of this experiment resemble those of mixed clouds in which vapor and the supercooled water droplets coexist because of the temperature range (−12 to −15 °C) and supersaturation of water vapor (a sufficient supply of vapor exists because of water evaporation from the water pans). Curves of the saturation vapor density over the water (C_{sw}) and saturation vapor density over ice (C_{si}) are shown in Fig. 1b to illustrate the variation history of water density by the equipment. The difference

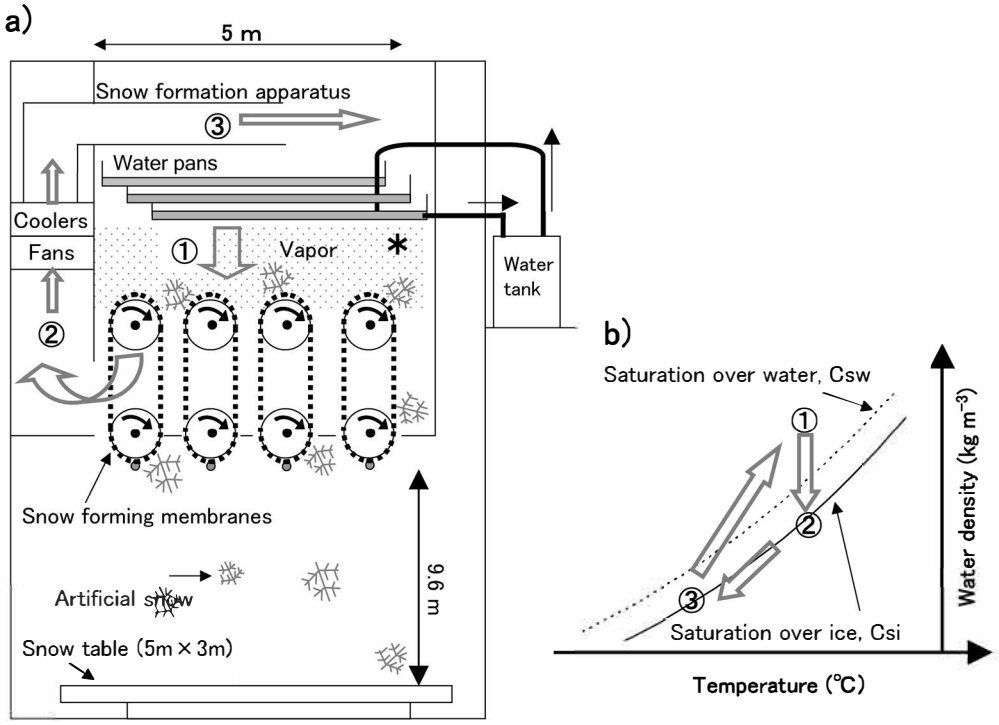

Fig. 1. (a) Schematic of the snow formation apparatus and (b) the variation history of water density change in the apparatus. Measuring point of the air temperature at the snow-forming apparatus (asterisk). The horizontal axis indicates air temperature and the vertical axis shows the water density. Curves of the saturation vapor density over water (C_{sw}) and the saturation vapor density over ice (C_{si}) are shown.

between C_{si} and C_{sw} plays a crucial role in accelerating snow formation. The process through which the snow is generated under the vapor supersaturation condition is termed the Bergeron-Findeisen process (Ciais and Jouzel, 1994). This snow-crystal growth process occurs in environments in which supercooled water droplets exist in the clouds. In such an environment, the supercooled water droplets may evaporate (a supercooled water droplet is one that is unsaturated over water); a snow crystal grows rapidly by absorbing the surrounding vapor (the vapor is supersaturated over ice).

2.2. *Experimental conditions*

We sampled the generated ice crystal, source vapor, and water in water pans under different conditions and recorded the temperature at the snow-forming membrane, temperature of the water pans and the snow accumulation rate (Table 1). The air temperature at the snow table was fixed at -15°C during the experimental period. The water circulated through the water pans and the storage tank with pipes; no water was supplied from outside during the experimental period. Four experiments were performed at the snow-forming membrane over four days, (hereafter, these four days are respectively expressed as A1, A2, A3, and A4) at a fixed temperature (-13°C) of the snow formation apparatus. A separate experiment was performed for one day (hereafter, B1) at a fixed temperature (-15°C) of the snow formation apparatus. Although ice crystals were produced continuously throughout the day during the experimental period, production was suspended in the afternoon of A3 for maintenance. The experiment was restarted after the equipment had been run for 5 h.

The supersaturation ratio was calculated using the observed snow accumulation rate and the airflow rate (Umezawa and Seki, 1997).

$$S_i = C_w / C_{si}. \tag{1}$$

In the above equation, S_i represents the supersaturation ratio over ice, C_{si} is the vapor

Table 1. Experimental conditions.

	Experiment A				Experiment B
Quantity	A1	A2	A3	A4	B1
Air temperature at snow formation apparatus (°C)	-13.8 ± 1.1	-13.8 ± 1.1	-13.8 ± 1.1	-13.8 ± 1.1	-18.6 ± 1.2
Air temperature at snow table (°C)	-15.0 ± 0.2	-15.0 ± 0.1	-15.0 ± 0.2	-15.0 ± 0.2	-15.0 ± 0.2
Water temperature of vapor source (°C)	20.2 ± 0.1	20.0 ± 0.1	24.5 ± 0.1	29.0 ± 0.1	20.1 ± 0.1
Snow accumulation rate ($kg\,h^{-1}\,m^{-2}$)	0.09	0.31 ± 0.01	0.72 ± 0.15	1.18 ± 0.05	0.72 ± 0.05
Rotation speed of snow-formation apparatus (h^{-1})	0.20	0.20	0.60	1.00	0.20
Super saturation ratio, S_i ($=C_w/C_{si}$)	1.031	1.106 ± 0.003	1.245 ± 0.052	1.405 ± 0.016	1.382 ± 0.029
Effective super saturation ratio, S_i' ($=C_{sw}/C_{si}$)	—	—	1.165 ± 0.013	1.165 ± 0.013	1.221 ± 0.014

density saturated over ice at the snow-forming membrane ($kg\,m^{-3}$), and C_w is the total water (liquid and vapor states) density at the snow-forming membrane ($kg\,m^{-3}$). The value of C_{si} is calculated from the air temperature in the snow-formation apparatus. This measuring point of air temperature is located above the snow-forming membrane (Fig. 1a). The air temperature at the snow crystals would be higher than the temperature at the C_{si} measuring point because of the latent heat release during crystal growth. However, we assume that the increase in temperature near the snow crystals is negligible because the incessant wind circulating through the gas-permeable membranes equalizes the temperature around the snow-forming membrane. We estimate C_w using the mass balance between the inflow and outflow of the snow-forming apparatus:

$$C_w \cdot G_f/\rho = G_S + C_{si} \cdot G_f/\rho. \quad (2)$$

Therein, G_f represents the mass flow of air calculated by the performance of fans of snow formation apparatus ($kg\,h^{-1}$), ρ is the dry-air density at the snow-forming membrane ($kg\,m^{-3}$), and G_S is the total of snow accumulation rate observed on he snowfall table ($kg\,h^{-1}$). The values of S_i in the experiments are presented in Table 1. Although the calculated values of C_w were larger than the value of C_{sw} in the A3, A4, and B1 experiments, the water vapor above C_{sw} exists in the form of supercooled water droplets (*e.g.*, Tusima, 2004). Because isotope fractionation from vapor to snow is dependent upon the amount of water in the vapor phase, we calculated the effective supersaturation ratio ($S_i' = C_{sw}/C_{si}$)—the theoretical maximum of the supersaturation ratio—in these experiments (Table 1).

2.3. Sampling and isotope analyses

The snow was sampled in eight plates of plastic pans (34 cm × 26 cm) placed on the snow table. The snow was collected and weighed approximately once hourly. It was then immediately transferred to a tight, sealed 100-m*l* screw bottle (Schott AG, Mainz, Germany). The water in the water pans, which supplies the water vapor, was sampled at intervals of 1 h for isotope measurements. The water was extracted using a syringe and put into a 10-m*l* bottle. The hydrogen and oxygen isotopic ratios analyses of snow and water in the water pans were measured using conventional equilibrium method (Horita *et al*., 1989) with an isotope ratio mass spectrometer (MAT252; Thermo Finnigan) installed at the Tokyo Institute of Technology. The analytical precisions (1σ) are 0.5‰ for δD and 0.05‰ for δ^{18}O.

The vapor was sampled cryogenically in the snow-formation apparatus. A vapor trap comprises a simple double-glass tube (Helliker *et al*., 2002). To cryogenically sample vapor in the snow formation apparatus, the following two provisions were made. First, because the air temperature is low, the collection was carried out not by dry-ice/ethanol bath, but by liquid nitrogen to increase the sampling efficiency. Second, the glass tubes we used are 12 mm and 9 mm diameter instead of 9 mm and 6 mm diameter. The flow rate was set between 2 and 2.5 *l* min^{-1} and sampling was carried out for approximately 1 h. The collected vapor had adhered to the upper end of the double tubes in the ice state. The adhered ice was slightly warmed manually to prevent the evaporation of water from heating with a gas burner during the sealing the glass tube and enable the evaporation of carbon dioxide. The ice sample was dropped into the

lower part of a pipe and the tube was sealed at the upper end using a gas burner.

The vapor sample that was sealed in the glass tube was moved to a smaller glass tube (6 mm diameter, 5–10 cm length) using a glass made vacuum line. Then, at room temperature, this sample was converted from ice into liquid water, which was put in a microvial (0.2 m*l*). The water was injected into a 1400°C pyrolysis furnace (TC/EA; Thermo Electron Corp., Bremen, Germany) under ultra-high purity helium flow using an auto-sampler (0.12 μl). Each water molecule was pyrolyzed into hydrogen and carbon monoxide in the furnace, then the isotope ratios were analyzed using an isotope ratio mass spectrometer (DELTA plus XP; Thermo Electron Corp.). The sample for which the isotopic ratio was known (melted iceberg) was prepared, and the difference after transfer by a glass vacuum line by glass tube pyrolysis and the above-mentioned isotope equilibrium method was determined using the same water sample. The isotopic ratios determined by the equilibrium method were $\delta D = -284.5 \pm 0.3‰$ ($n=10$) and $\delta^{18}O = -36.54 \pm 0.02‰$ ($n=10$); those determined by the pyrolysis method were $\delta D = -282.7 \pm 1.4‰$ ($n=6$) and $\delta^{18}O = -36.10 \pm 0.32‰$ ($n=6$). Although the analytical precision of the equilibrium method was better than that of the pyrolysis method, both results generally agreed within analytical errors.

3. Result

3.1. Produced artificial snow

Photographs of the produced artificial snow are shown in Fig. 2. Most ice crystals have a dendrite-like shape with adhering cloud droplets. In the low supersaturation ratio experiment (A1 and A2), the dendrite-like crystals with plates were observed and the snow density was 0.02–0.03 g cm^{-3}. In the high supersaturation ratio experiment (A3, A4, and B1), dendrite-like ice crystals with numerous adhering cloud droplets were

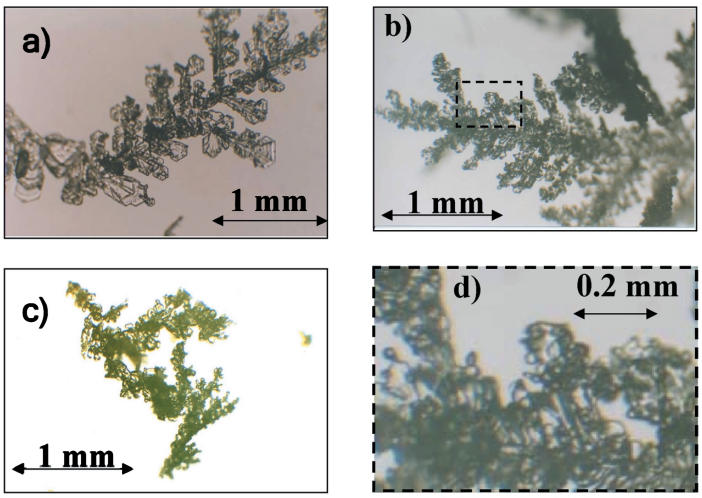

Fig. 2. Produced artificial snow under different conditions. Photographs of experimental conditions of a) A2, b) A4, and c) B1. d) A closer view of the area within the dotted square shown in b).

observed (Fig. 2d). The density of snow was 0.08–0.09 g cm^{-3}. The cloud droplets' respective diameters were 7–23 μm (avg. 13 μm). Assuming that droplets are spherical, the crystal mass is calculated using a formula that estimates the dendrite mass from the diameter of a circumscribed circle (Higuchi, 1956); the water droplet percentage of the snow crystal was 2–22%.

3.2. *Isotopic results*

Analytical results of the isotopic ratio for hydrogen and oxygen are shown in Table 2 along with the *d* value and the respective sampling times of snow and vapor samples. Overall, the snow isotopic ratio became heavier with time from experiments A1 to B1. This increase results from the increase in the isotopic ratio of the vapor source water in the water pans caused by the generation of isotopically light snow. At the end of the

Table 2. Isotope ratios of snow, vapor and water pan for respective experiments.

Snow					Vapor					Water pan			
Sampling time		Isotope ratio (‰)			Sampling time		Isotope ratio (‰)			Sampling	Isotope ratio (‰)		
Start	End	δD	$\delta^{18}O$	*d*	Start	End	δD	$\delta^{18}O$	*d*	time	δD	$\delta^{18}O$	*d*
Experiment A1													
15:53	17:13	-65.8	-20.43	97.6	16:16	17:38	-196	-37.5	104	15:20	-46.2	-7.04	10.1
										16:09	-45.6	-6.76	8.4
Average		**-65.8**	**-20.43**	**97.6**	**Average**		**-196**	**-37.5**	**104**	**Average**	**-45.9**	**-6.90**	**9.2**
1 σ		**-**	**-**	**-**	**1 σ**		**-**	**-**	**-**	**1 σ**	**0.3**	**0.14**	**0.8**
Experiment A2													
9:13	10:15	-46.8	-16.23	83.1	9:31	10:45	-159	-29.9	79	9:35	-24.8	-1.44	-13.3
10:26	11:25	-46.9	-15.87	80.1						10:35	-23.0	-0.98	-15.2
11:30	12:43	-44.9	-15.44	78.6						11:40	-22.4	-0.55	-18.0
12:53	13:43	-45.7	-15.49	78.2						12:58	-20.4	-0.01	-20.3
13:55	14:50	-48.2	-16.25	81.8						14:01	-21.5	-0.48	-17.6
										15:05	-20.1	-0.03	-19.8
Average		**-46.5**	**-15.86**	**80.4**	**Average**		**-159**	**-29.9**	**79**	**Average**	**-22.0**	**-0.58**	**-17.4**
1 σ		**1.3**	**0.39**	**2.1**	**1 σ**		**-**	**-**	**-**	**1 σ**	**1.6**	**0.51**	**2.5**
Experiment A3													
9:00	9:57	-48.0	-13.79	62.3	10:35	11:31	-167	-26.1	41	9:08	-6.3	4.03	-38.5
10:08	11:00	-40.0	-12.54	60.3	11:50	12:43	-172	-25.7	33	10:15	-3.8	4.57	-40.3
11:08	11:59	-40.7	-12.54	59.6	13:10	14:15	-170	-26.0	38	11:15	-2.3	4.99	-42.3
12:48	13:40	-46.5	-13.38	60.5						12:55	-4.6	4.34	-39.3
										13:57	-2.1	4.88	-41.2
Average		**-43.8**	**-13.06**	**60.7**	**Average**		**-170**	**-25.9**	**37**	**Average**	**-3.8**	**4.56**	**-40.3**
1 σ		**3.5**	**0.54**	**1.0**	**1 σ**		**2**	**0.2**	**3**	**1 σ**	**1.5**	**0.35**	**1.3**
Experiment A4													
9:53	10:53	-50.3	-14.14	62.8	11:58	12:58	-175	-25.9	33	10:40	-4.3	4.50	-40.3
11:06	12:03	-44.9	-13.21	60.7	13:12	14:14	-172	-25.1	29	11:40	-1.3	5.21	-43.0
12:38	13:39	-43.3	-12.44	56.2	14:25	16:34	-165	-25.1	36	12:55	1.9	6.01	-46.2
13:48	14:49	-41.0	-11.73	52.8						14:10	4.6	6.88	-50.5
14:58	15:46	-39.0	-11.23	50.9						15:28	2.8	6.48	-49.0
Average		**-43.7**	**-12.55**	**56.7**	**Average**		**-170**	**-25.4**	**33**	**Average**	**0.7**	**5.81**	**-45.8**
1 σ		**3.8**	**1.03**	**4.5**	**1 σ**		**4**	**0.4**	**3**	**1 σ**	**3.2**	**0.86**	**3.8**
Experiment B1													
9:03	10:01	-45.3	-10.85	41.4	11:00	12:03	-184	-24.5	12	9:35	12.1	8.73	-57.8
10:09	11:09	-44.9	-10.61	40.0	12:17	13:20	-174	-24.0	18	10:43	14.3	9.24	-59.7
11:17	12:20	-45.6	-10.79	40.7						12:01	10.5	8.03	-53.8
12:29	13:37	-43.8	-10.51	40.2						13:18	11.8	8.54	-56.5
Average		**-44.9**	**-10.7**	**40.6**	**Average**		**-179**	**-24.3**	**15**	**Average**	**12.2**	**8.64**	**-56.9**
1 σ		**0.7**	**0.14**	**0.5**	**1 σ**		**5**	**0.2**	**3**	**1 σ**	**1.4**	**0.44**	**2.2**

experiment, the isotopic ratios of the water in the water pans became heavier (δD, +58.1‰; δ^{18}O, +15.54‰) and the d values became lighter (d, −66.1‰) than their initial values (Table 2).

In this experiment, the vapor used as raw material for the snow was produced as follows: (1) supplied from the water pans, (2) re-circulated after snow formation, and (3) passed in and out to the apparatus exterior. Therefore, the Rayleigh distillation process, by which the snow produced in the closed system is removed completely from the system, is inapplicable to this experimental result. Assuming that the conditions in each experiment (A1–A4, B1) are constant for a day, the daily average values were adopted for further discussion. In other words, the changes in the isotope ratio of the water in the water pans within a day were ignored. Errors (1σ) arising from this assumption are 1–5‰ for δD, 0.1–1.0‰ for δ^{18}O, and 1–5‰ for d (Table 2).

4. Discussion

We first compared our results with the previous experiment on snow formation performed at room temperature by Jouzel and Merlivat (1984). Subsequently, other physical factors that affect measurement results, such as a supercooled water droplets and sublimation of snow after the snowfall, were calculated. The changes in the d values were estimated, as presented in the following sections. Experimental results suggest that the snow formation process in the supersaturation condition affects the kinetic isotope fractionation of water.

4.1. Comparison with previous study

Jouzel and Merlivat (1984) (hereafter, JM84) indicated the existence of the isotope effect by molecular diffusion in the case of ice crystal growth. Isotope fractionation from vapor to ice crystals is determined by two mechanisms: phase equilibrium of ice-vapor and molecular diffusivity of water isotopes. The kinetic fractionation factor from vapor to ice, α_{ki}, is expressed as

$$\alpha_{ki}=\alpha_{i-v}\alpha_k \quad \text{with} \quad \alpha_k=\frac{S_i}{\alpha_i(D/D')(S_i-1)+1}, \tag{3}$$

$$\delta_{\text{ice crystal}}\times 10^{-3}+1=\alpha_{i-v}\alpha_k\cdot(\delta_{\text{vapor}}\times 10^{-3}+1). \tag{4}$$

In the above equations, α_{i-v}, equilibrium fractionation factor; α_k, kinetic fractionation factor; D/D', molecular diffusivity ratio, $D(HDO)/D(H_2O)=0.9755$, $D(H_2{}^{18}O)/D(H_2{}^{16}O)=0.9723$ (Merlivat, 1978). Details of this equation are described in JM84. That study measured the isotopic ratio of the frost grown on a low-temperature plate (−20°C) set at room temperature environment (20°C) to validate the existence of the kinetic isotope effect.

Our experimental results and those of JM84 are shown in Fig. 3. The influence of the supercooled droplets on the isotope ratios is ignored at this point and will be discussed in the following section. The influence of the supercooled droplets does not affect the inferences drawn in this Discussion section. The snow isotope values shown in Fig. 3 were calculated based on the observed isotope fractionation factors. For this calculation, we arbitrarily chose the vapor isotope ratio of experiment A3 as the initial

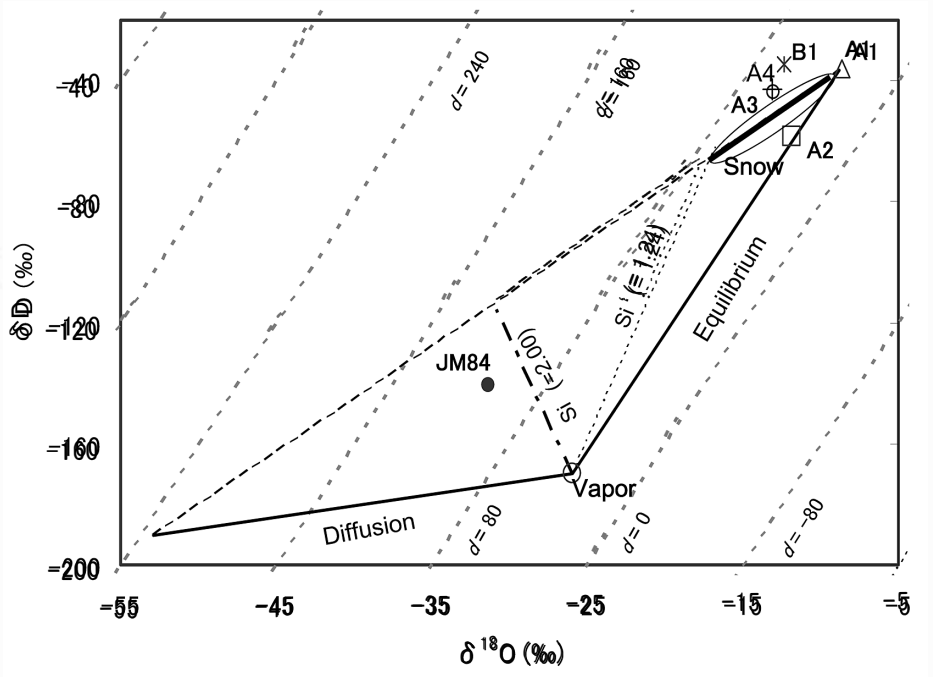

Fig. 3. Experimental results of vapor and snow isotope ratios. The snow isotope ratio of A1 (open triangle), A2 (open square), A3 (open circle), A4 (cross), B1 (asterisk), and the results obtained by Jouzel and Merlivat (1984) (JM84, closed circle). All isotope ratios of snow are calculated using their fractionation factors with the vapor isotope ratio of A3 as their initial value. Each solid line shows the pure equilibrium fractionation at −13.8°C, pure diffusional fractionation, the theoretical fractionation at the maximum S_i' ($=1.24=e_{sw}/e_{si}$) at −20°C (dotted line), and the theoretical fractionation at the S_i ($=2.00$) (dashed dotted line). Snow isotopic ratios will fall on the line (encircled bold solid line) between the end of equilibrium fractionation ($S_i=1$) and that of the fractionation at the maximum supersaturation ratio ($S_i'=e_{sw}/e_{si}$). Gray dotted-slash lines represent iso-d lines ($d=\delta D-8\cdot\delta^{18}O$).

value. The equilibrium fractionation factor at −13.8°C was used for drawing the equilibrium fractionation line. With the exception of A1 and A2, which had low S_i, the slopes of $\delta D/\delta^{18}O$ in other experiments (A3, A4, B1) shifted from the equilibrium fractionation line. This slope is predicted when S_i is set at 1.17. This value is close to the observed S_i'. On the other hand, the result of JM84 is near the line when $S_i=2.00$ at the crystal growing temperature of −20°C, which is greater than the upper limit value of S_i' ($=1.24$) at this temperature. This fact suggests that their experiment did not simulate isotope fractionation during snow formation in the clouds.

Major differences between the experimental conditions of JM84 and those of the present study include the following: (1) because the experiment of JM84 is conducted at room temperature, the temperature gradient of the cooling plate is large; and (2) dominance of the molecular diffusive transport exists because the wind speed in a crystal growth area is very low in the JM84 experiment. Both conditions cause a large apparent supersaturation ratio because they enhance the molecular diffusive transport and the

layer at which molecular diffusion predominates would be thick. For example, assuming that the upper end temperature of a molecular diffusion layer is -14°C, the obtained apparent "S_i" ($=C_{sw}$ at -14°C/C_{si} at -20°C) is two, thereby explaining the experimental result of JM84.

4.2. Quantitative estimation of results

We quantitatively estimated the isotope fractionation processes that affect the experiment. Thereby, we compare the experimental results with the theoretical estimation. First, the error of the experimental result was estimated based on the influence of the supercooled water droplets of the vapor sample. Using this isotope ratio of vapor as an initial value, the theoretical snow isotopic ratio was calculated considering three processes: (1) kinetic fractionation from vapor to ice crystals (JM84); (2) the freezing of supercooled water droplets onto the ice crystals; and (3) sublimation of snow after snowfall.

Supercooled water droplets might exist at high supersaturation conditions. In our experiment, vapor sampling included the sampling of these droplets with vapor. The observed isotope ratio of the vapor sample including droplets ($\delta_{\text{vapor measured}}$) was expressed by isotope ratios of supercooled droplets (δ_{droplets}), that of vapor (δ_{vapor}), and the mole fraction (k).

$$\delta_{\text{vapor measured}} = k \cdot \delta_{\text{vapor}} + (1-k) \cdot \delta_{\text{droplets}}. \tag{5}$$

An upper limit of k is estimated using the saturation vapor pressure over water when the vapor amount is higher than the saturation vapor pressure over water. In general, this is the most common situation that we considered. On the other hand, a lower limit value is obtained in the case in which the vapor amount is equivalent to the amount of saturation pressure over ice. In other words, all water above the saturation of ice exists as supercooled water droplets. In this case, the amount of vapor is underestimated because most water exists as vapor under the saturation vapor pressure over water. However, the photographs showed a small quantity of supercooled droplets under saturation conditions (A1 and A2). Then the possibility exists that supercooled droplets locally existed below the saturation vapor pressure over water.

The isotopic ratio of cloud droplets (δ_{droplets}) is estimated as follows. Observed diameters of water droplets frozen on an ice crystal are less than 23 μm. Droplets of such diameters were achieved at isotopic equilibrium with surrounding vapor within a short period of time (<30 s) (Jouzel *et al*., 1975). In this experiment, the isotopic ratio of a cloud droplet (δ_{droplets}) was calculated assuming the isotopic equilibrium with a surrounding vapor (δ_{vapor}) (eq. 6). The pseudo-equilibrium condition (Ciais and Jouzel, 1994) at low supersaturation conditions (A1 and A2) was not considered:

$$\delta_{\text{droplets}} \times 10^{-3} + 1 = \alpha_{w-v} \cdot (\delta_{\text{vapor}} \times 10^{-3} + 1), \tag{6}$$

where α_{w-v}, the equilibrium fractionation factor between water and vapor.

Theoretical estimation of snow isotope value ($\delta_{\text{snow sam}}$) was determined by the following set of equations. In addition to the kinetic fractionation from vapor to ice crystals (eq. 4), the isotope values of snow in this experiment are affected by two factors: freezing of supercooled water droplets onto the ice crystals and evaporative sublimation

after snow formation on the snow table. The isotope fractionation of the freezing of water droplets was negligible because of the rapid freezing rate (Ciais and Jouzel, 1994). The isotope value of ice crystals to which droplets were adhered ($\delta_{\text{ice and droplets}}$) is expressed as

$$\delta_{\text{ice and droplets}} = \delta_{\text{ice crystal}} \cdot (1-p) + \delta_{\text{droplets}} \cdot (p), \tag{7}$$

where $\delta_{\text{ice crystal}}$, theoretical isotope value of ice crystal (eq. 4); p, the mass ratio of frozen supercooled droplets onto the ice crystals. The quantity of the supercooled water droplets adhering to the snow was estimated using a photograph; its maximum value of 22% (details in the Results section) was adopted for estimation. Second, the isotopic ratio of the snow that we sampled on the snow table ($\delta_{\text{snow sam}}$) was probably influenced by sublimation during snow sampling (*ca*. one hour): the humidity around the snow table of our experimental apparatus was low because of the use of a defroster. This sublimation effect can be expressed with a Rayleigh model:

$$\delta_{\text{snow sam}} \times 10^{-3} + 1 = (\delta_{\text{ice and droplets}} \times 10^{-3} + 1) \cdot f^{(\alpha_{\text{i-v}}-1)}. \tag{8}$$

In that model, $\alpha_{\text{i-v}}$ is the equilibrium fractionation factor between ice and vapor and f is the fraction of snow remaining. The sublimation rate per unit area was calculated from the measuring mass change in the snow after snowfall to estimate the amount of sublimation. The artificial snow in a plastic dish was put on the snow table with a cover to prevent additional accumulation. It was weighed a few hours later with an electrobalance; its mass change was $0.012\,\text{kg}\,\text{m}^{-2}\,\text{h}^{-1}$. For each experiment, the amount of sublimation was calculated based on the sampling time of snow and the sublimation rate. The estimated ratios of sublimation for each sampling were 1–13%. However, this value is the maximum estimate. The snow hardly thaws in the experiment. For that reason, the water molecules of residual snow would not be mixed well. Consequently, the possibility exists that the isotope ratios of snow did not change during sublimation.

4.3. Changes in deuterium excess

We considered experimental results using variations in the d value because d is a suitable index for examining how water isotope ratios depend on the vapor supersaturation ratio (S_{i}). In consideration of the above effect, a change in the d value from vapor to snow, Δd ($=d_{\text{snow}}-d_{\text{vapor}}$), is shown in Fig. 4 along with the experimental conditions. The estimated error of the influence of the water droplets during vapor sampling on Δd (± 1‰) is smaller than the analytical error of the d value (± 2.9‰). The experimental result of Δd proves the existence of the kinetic isotope effect. Theoretical estimation of Δd is low under conditions of lower supersaturation (close to the isotope equilibrium) and high under higher supersaturation ratio conditions. An increase in Δd along with higher supersaturation conditions (Fig. 4) in the experimental results are in agreement with that prediction.

In this paper, the diffusional fractionation factor of Merlivat (1978) was adopted for calculations because it is the most widely adopted factor in Antarctic studies. However, a recent study (Cappa *et al*., 2003) proposed revised fractionation factors of molecular diffusion that differ considerably from Merlivat's value. Results of Δd obtained using these new diffusion coefficients are shown in Fig. 4. The Δd calculated

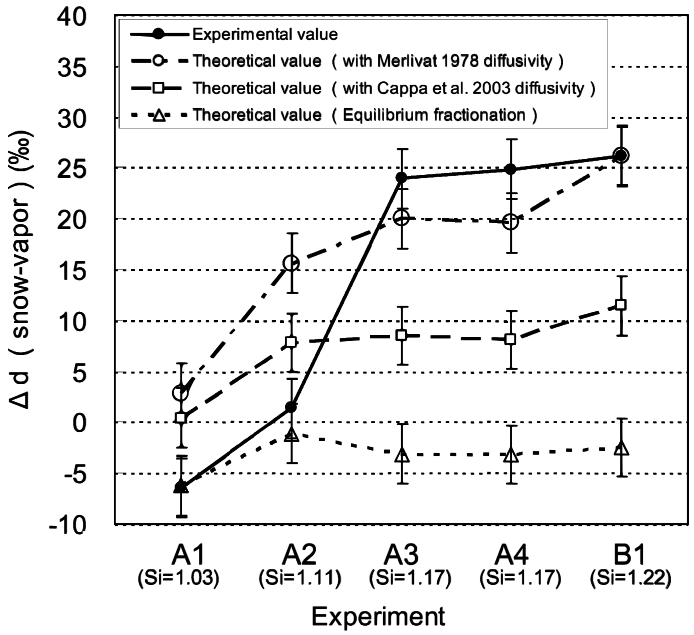

Fig. 4. The difference between deuterium excess of vapor and that of snow. The horizontal axis indicates experimental conditions; the vertical axis shows the variation of deuterium excess from vapor to snow Δd ($=d_{snow}-d_{vapor}$) (see text). Each symbol shows the results of this experiment (closed circle), the theoretical values calculated with equilibrium fractionation (open triangles), the theoretical values calculated with molecular diffusivities of Merlivat (1978) (open circles), and Cappa et al. (2003) (open squares).

by the diffusional coefficients of Cappa *et al*. (2003) is smaller than that of Merlivat (1978). Results of Δd using the diffusional coefficients of Cappa *et al*. (2003) in the experiments A3 and A4 are 11‰ smaller than that of Merlivat (1978). Figure 4 shows that our experimental results of Δd are closer to the estimated Δd values using coefficients of Merlivat (1978) than that of Cappa *et al*. (2003). Therefore, the result of our experiment is more consistent with that of Merlivat (1978).

4.4. Limitation of this study and implications for ice core analysis

Although the wind blows in the direction of the snow crystals because of the gas-permeable membrane of the snow-formation apparatus, the ventilation coefficients of our experiment are different from that of a free-fall condition that is prevalent in the clouds. However, the isotopic effect caused by ventilation coefficients is expected to be small for the hollow column-type ice crystals (Jouzel and Merlivat, 1984). A convection-type artificial snow experiment would be promising for verifying the effect of ventilation coefficients. A typical limitation of such an experiment is the amount of sample required for isotopic analysis. Our vapor sampling method is not ideal for the experiment because it requires long pumping (about one hour) and would suffer carbon-dioxide contamination. However, a recently developed method that requires nanomole

quantities of water for hydrogen-isotope analysis (Eiler and Kitchen, 2001) offers the potential to perform experiments more precisely in small systems.

A model calculation that reproduces d values of snow in inland Antarctica is widely used to interpret the d record of the Antarctic ice core (*e.g.*, Vimeux *et al.*, 2001). The result of our experiment suggests the existence of kinetic fractionation during ice crystal growth. Therefore, although a model for considering only the effect of eddy diffusion exists (Hendricks *et al.*, 2000), one that considers both the eddy diffusion and snow formation (Kavanaugh and Cuffey, 2003) is more appropriate for d studies in Antarctica.

5. Conclusions

We measured the isotope ratios of snow and vapor under a controlled temperature to verify the kinetic effect during the snow-formation process. We also measured the vapor supersaturation ratio using a large-scale artificial snow machine. This is the first experiment to verify the theoretical formula of kinetic fractionation during snow formation proposed by Jouzel and Merlivat (1984). Experimental results of deuterium excess were compared with theoretical estimation by considering the effect of supercooled droplets during vapor sampling and the secondary effect on snow (sublimation and freezing of droplets). Although this estimation depends on molecular diffusivities (Merlivat, 1978; Cappa *et al.*, 2003), our experimental results show rough agreement with the theoretical results obtained using the coefficients obtained by Merlivat (1978). These results suggest the validity of kinetic fractionation during snow formation. This effect should be taken into consideration when calculating the d value for the Antarctic snow.

Acknowledgments

We thank M. Seki and I. Ohta (Toyo Engineering Works Ltd.) for technical information provided regarding the snow-formation apparatus. We are grateful to K. Fujii, M. Sato (New Energy and Industrial Technology Development Organization), and K. Yamada (Tokyo Institute of Technology) for isotopic analyses by TC/EA-IRMS, and to O. Abe (Nagoya University), N. Kurita (Frontier Observational Research System for Global Change), and T. Takahashi (Hokkaido University of Education) for advice at the beginning of this experiment. This study is a joint research project of the Tokyo Institute of Technology and the National Research Institute for Earth Science and Disaster Prevention. It was partly supported by a Grant-in-Aid for JSPS Fellows, JSPS Research Fellowships for Young Scientists and Japan Science and Technology Agency.

References

Cappa, C.D., Hendricks, M.B., DePaolo, D.J. and Cohen, C. (2003): Isotopic fractionation of water during evaporation. J. Geophys. Res., **108** (D16), 4525, doi: 10.1029/2003JD003597.

Ciais, P. and Jouzel, J. (1994): Deuterium and oxygen 18 in precipitation: Isotopic model, including mixed cloud processes. J. Geophys. Res., **99**, 16793–16803.

Dansgaard, W. (1964): Stable isotopes in precipitation, Tellus, **16**, 436–468.
Eiler, J.M. and Kitchen, N. (2001): Hydrogen-isotope analysis of nanomole (picoliter) quantities of H_2O. Geochem. Cosmochim. Acta, **65**, 4467–4479.
Helliker, B.R., Roden, J.S., Cook, C. and Ehleringer, J.R. (2002): A rapid and precise method for sampling and determining the oxygen isotope ratio of atmospheric water vapor. Rapid Commun. Mass Spectrom., **16**, 929–932.
Hendricks, M.B., Depaolo, D.J. and Cohen, R.C. (2000): Space and time variation of $\delta^{18}O$ and δD in precipitation: Can paleotemperature be estimated from ice cores? Global Biogeochem. Cycles, **14**, 851–861.
Higashiura, M., Abe, O., Sato, T., Numano, N., Sato, A., Yuuki, H. and Kosugi, K. (1997): Preparation of an experimental building for snow and ice disaster prevention. Snow Engineering-Recent Advances, ed. by M. Izumi *et al*. Rotterdam, A.A. Balkema, 605–608.
Higuchi, K. (1956): A new method for the simultaneous observation of shape and size of a large number of falling snow particles. J. Meteorol., **13**, 274–278.
Horita, J., Ueda, A., Mizukami, K. and Takatori, I. (1989): Automatic δD and $\delta^{18}O$ analyses of multi-water samples using H_2- and CO_2-water equilibration methods with a common equilibration set-up. Appl. Radiat. Isot., **40**, 801–805.
Jouzel, J. and Merlivat, L. (1984): Deuterium and oxygen 18 in precipitation: Modeling of the isotopic effects during snow formation. J. Geophys. Res., **89**, 11749–11757.
Jouzel, J., Merlivat, L. and Roth, E. (1975): Isotopic study in hail. J. Geophys. Res., **80**, 5015–5030.
Kavanaugh, J.L. and Cuffey, K.M. (2003): Space and time variation of $\delta^{18}O$ and δD in Antarctic precipitation revisited. Global Biogeochem. Cycles, **17** (1), 1017, doi: 10.1029/2002GB001910.
Merlivat, L. (1978): Molecular diffusivities of $H_2{}^{16}O$, $HD^{16}O$, and $H_2{}^{18}O$ in gases. J. Chem. Phys., **69**, 2864–2871.
Nakaya, U. (1951): The formation of ice crystals. Compendium of Meteorology, Boston, Am. Meteorol. Soc., 207–220.
Stenni, B., Masson-Delmotte, V., Johnsen, S., Jouzel, J., Longinelli, A., Monnin, E., Röthlisberger, R. and Selmo, E. (2001): An oceanic cold reversal during the last deglaciation. Science, **293**, 2074–2077.
Tusima, K. (2004): Problems of Nakaya's diagram and diffusion cloud chamber for growing ice crystals. Tenki, **51**, 753–758.
Uemura, R., Yoshida, N., Kurita, N., Nakawo M. and Watanabe, O. (2004): An observation-based method for reconstructing ocean surface changes using a 340,000-year deuterium excess record from the Dome Fuji ice core, Antarctica. Geophys. Res. Lett., **31** (13), L13216, doi: 10.1029/2004GL019954.
Umezawa, K. and Seki, M. (1997): Large quantities snow making of singular crystal (rotation ventilation filter method). Kanchi Gijutu Symposium (Proc. 13th Cold Region Tech. Conf.), Sapporo, Hokkaido Development Engineering Center, 12–16.
Vimeux, F., Masson, V., Delaygue, G., Jouzel, J., Petit, J.R. and Stievenard, M. (2001): A 420,000 year deuterium excess record from East Antarctica: Information on past changes in the origin of precipitation at Vostok. J. Geophys. Res., **106**, 31863–31873.
Watanabe, O., Jouzel, J., Johnsen, S., Parrenin, F., Shoji, H. and Yoshida, N. (2003): Homogeneous climate variability across East Antarctica over the past three glacial cycles. Nature, **422**, 509–512.